Landslide-dammed paleolake perturbs marine sedimentation and drives genetic change in anadromous fish

Benjamin H. Mackey[a,1,2], Joshua J. Roering[a], and Michael P. Lamb[b]

[a]Department of Geological Sciences, 1272 University of Oregon, Eugene, OR 97403; and [b]Division of Geological and Planetary Sciences, California Institute of Technology, 1200 East California Boulevard, Pasadena, CA 91125

Large bedrock landslides have been shown to modulate rates and processes of river activity by forming dams, forcing upstream aggradation of water and sediment, and generating catastrophic outburst floods. Less apparent is the effect of large landslide dams on river ecosystems and marine sedimentation. Combining analyses of 1-m resolution topographic data (acquired via airborne laser mapping) and field investigation, we present evidence for a large, landslide-dammed paleolake along the Eel River, CA. The landslide mass initiated from a high-relief, resistant outcrop which failed catastrophically, blocking the Eel River with an approximately 130-m-tall dam. Support for the resulting 55-km-long, 1.3-km³ lake includes subtle shorelines cut into bounding terrain, deltas, and lacustrine sediments radiocarbon dated to 22.5 ka. The landslide provides an explanation for the recent genetic divergence of local anadromous (ocean-run) steelhead trout (*Oncorhynchus mykiss*) by blocking their migration route and causing gene flow between summer run and winter run reproductive ecotypes. Further, the dam arrested the prodigious flux of sediment down the Eel River; this cessation is recorded in marine sedimentary deposits as a 10-fold reduction in deposition rates of Eel-derived sediment and constitutes a rare example of a terrestrial event transmitted through the dispersal system and recorded offshore.

erosion | Franciscan mélange | genetic introgression

Rivers are a crucial link between terrestrial and marine environments, facilitating the transfer of water, sediment, carbon, and solutes to the oceans (1–3), while providing a bidirectional corridor for the movement of animals and nutrients (4). Although fluvial processes that facilitate these functions are usually envisioned as continuous, large river-blocking landslides can have punctuated and persistent effects on the form, sediment-transport capacity, and habitability of river networks. Landslide debris and associated reservoir sedimentation can reside in the channel for >10⁴ years (5–8), and the effects of large landslides on the landscape and river habitat can persist long after the landslide mass is removed (9–11). Less apparent is the long-term legacy of landslides on ecosystem dynamics and offshore sediment dispersal because it can be difficult to relate these secondary effects, which can have a broad geographic scope, to specific paleolandslide events.

Owing to high rates of erosion (1, 2, 12–14), endangered redwood forests, 20th century floods (13, 15), vast land-use effects (1), minimal engineered damming (13), and a proximal marine depocenter (16–18), the Eel River, CA (Fig. 1) is one of the most intensively studied fluvial-marine systems in the world. Characterized by weak, highly sheared accretionary mélange rock prone to slope instability (12, 14), active tectonics associated with the Mendocino triple junction (19, 20), and high seasonal peak discharges (15, 21), the Eel River boasts the highest sediment yield of any nonglacial river in the contiguous United States (13). Extensive slow-moving landslides and gully systems dominate modern sediment production, producing readily transportable material that is rapidly conveyed to coastal and marine environ-

ments (12–14). Although these geomorphic processes promote efficient sediment delivery and downstream conveyance, analysis of offshore sediment provenance reveal highly anomalous patterns in the late Pleistocene (16), suggesting that the Eel River experienced a major (order-of-magnitude) decrease in sediment yield. This time also corresponds to a genetic divergence between ecotypes of anadromous steelhead fish (22), a divergence regionally unique to Eel River populations.

Here, we present evidence for a hitherto unknown late Pleistocene landslide-dammed paleolake on the main stem Eel River. This event can reconcile the anomalies observed in both fish genetics and marine sedimentation, and it demonstrates a direct link between a profound but relatively short-lived geological event and a persistent ecological response.

Results and Discussion

Using a 230-km², 1-m resolution Light Detection and Ranging (LiDAR) dataset along a 30-km stretch of the Eel River (Fig. 1), we observe extensive earthflow activity generating long, gently sloping (30–35%) hillslopes (14) with sparse terraces flanking the main channel. However, an abundance of subtle, near-horizontal surfaces identified on the LiDAR dataset (Figs. S1–S3) occur at a relatively consistent elevation (240- to 243-m above sea level). These features contrast with typical river terrace profiles, including some documented along the nearby South Fork Eel River (23, 24), which tend to decrease in elevation downstream tracing paleoriver beds. The bench-like features in our study area are typically gently undulating surfaces with bioturbated, fine-grained sediments and occasional gravel clasts. A LiDAR-based hypsometric analysis reveals a pronounced increase in planform area at 239–243 m elevation when compared to the background trend (Fig. 2). The increased area between 239 and 244 m (*ca.* 40,000 m²) is comparable to the approximate 38,000 m² cumulative area deficit within 245- to 250-m elevation. We interpret this hypsometric trend as morphologic evidence for shoreline features of a paleolake with stable water levels for a substantial period of time, causing slope truncation and shore platform formation. Further, small creeks and gullies at approximately 240 m commonly exhibit a wedge of fine-grained sediments indicating deltaic sedimentation into the lake (Figs. S2–S3). Analysis of the Eel River long profile shows a slight convexity at the upstream portion of the lake (Fig. S4), suggesting either substantial sediment deposition, or reduced channel incision due to armoring of the channel bed by standing water or sediment (9).
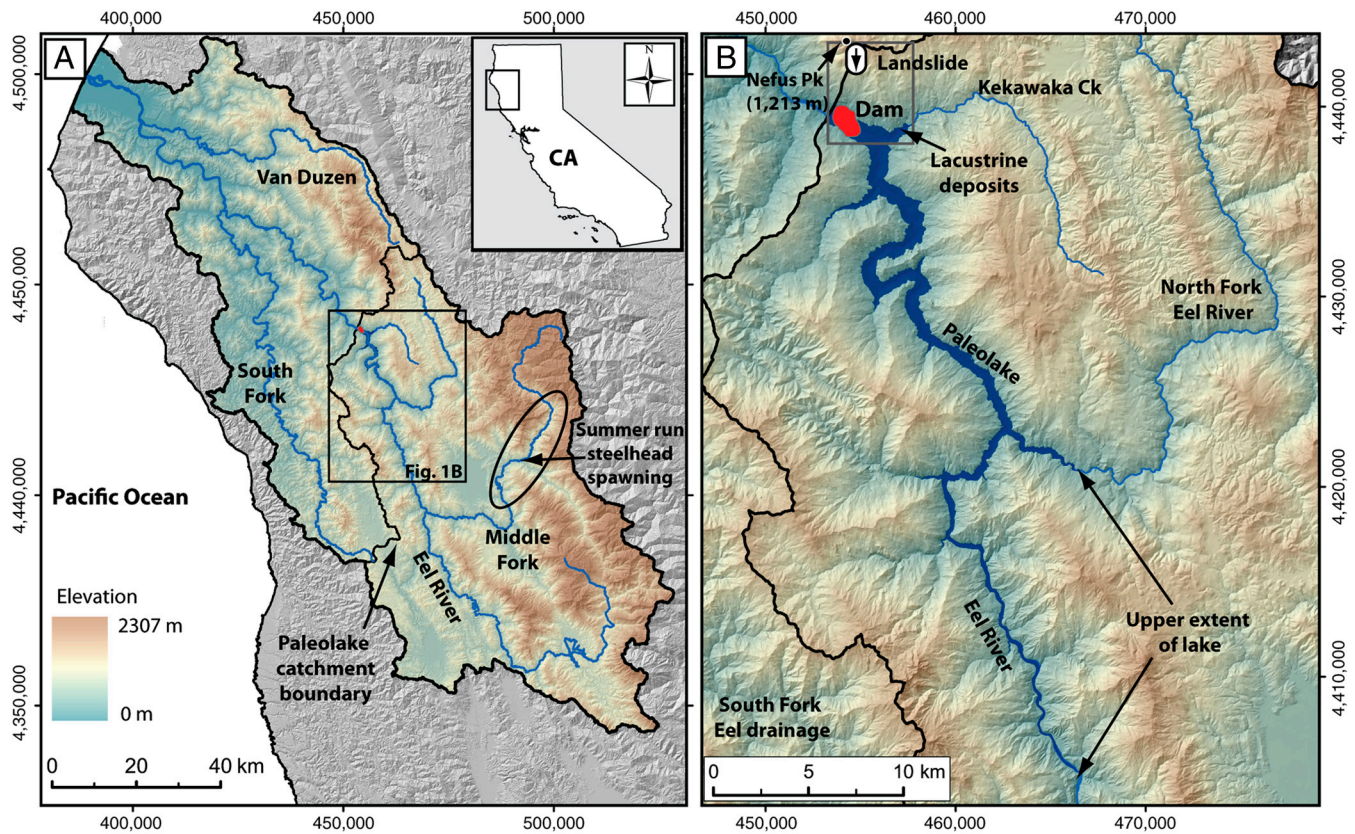
GEOLOGY

EVOLUTION

Fig. 1. (*A*) Eel River catchment showing major tributaries and the extent of the paleolake catchment. Inset shows location in northern California. (*B*) Paleolake extent along the main stem Eel River. Approximate dam location is shown in red. Gray box indicates extent of Fig. 3. Coordinates are Universal Transverse Mercator Zone 10N.

Pivotal to the landslide-dammed paleolake hypothesis is identification of a landslide capable of damming the Eel River. We identified a large 0.8-km², *ca.* 100-m-deep landslide scar (25) on the southwestern flank of Nefus Peak (Fig. 3), a heavily forested, approximately 5-km² high-relief (1,213 m) greenstone outcrop composed of mafic *meta*-igneous rock (25). The landslide scar has a steep-sided, elongate-scoop morphology characteristic of a rapidly moving translational landslide (26), in sharp contrast to the gentle, fluid appearance of the surrounding earthflow-prone terrain (14) (Fig. 3). The landslide scar has a minimum estimated volume of 3.6×10^7 m³, whereas the estimated minimum volume

of the dam is 2.0×10^7 m³. Based on a water surface elevation of 240 m and modern riverbed elevation below the landslide scar (*ca.* 100 m), the dam would have been up to 140-m high. We could not locate any other potential landslide sources capable of damming the Eel River to the 240-m elevation downstream of Nefus Peak, whereupon the valley widens, and mean local relief decreases (Fig. 1 and Fig. S4).

Landslide-dammed lakes commonly exhibit delta features and lacustrine sediments (27, 28). We discovered an outcrop of laminated sediments on the southern bank of Kekawaka Creek (Figs. 1*B*, 3, and 4) at 230 m above sea level, 10 m below the purported lake surface. The exposure consists of decimeter-scale alternating packages of fine sandy silt and coarse gravel sequences, with 2.5 m of total vertical exposure (Fig. 4*A*). The fine-grained packages are submillimeter scale laminated sandy silts and clays, with intricate fluid-escape structures (Fig. 4*B*), indicating suspension fall out (29). Such deposits are typical of a lacustrine environment and river-fed basins (30), but are foreign to an uplifting, highly erosive landscape such as the upper Eel River catchment.

Radiocarbon dating of wood and detrital charcoal within the lower fine silt layers returned a range of radiocarbon ages (Table S1). Two intact bark and wood samples have modern ages and likely reflect recent penetration of the sediments by roots. Three detrital charcoal samples returned calendar (31) ages of 22.6, 25.7, and 41.3 ka. Detrital charcoal should be assumed a maximum age given the potential for charcoal to reside in soils prior to deposition. Therefore, as there are samples close in age at 22.6 and 25.7 ka, these dates more likely represent the timing of deposition than the older age that exceeds 40 ka.

Although little morphologic evidence for a dam is preserved below the landslide scar, given the approximate timing of the landslide dam (*ca.* 22.5 ka) and long-term erosion rates (approxi-
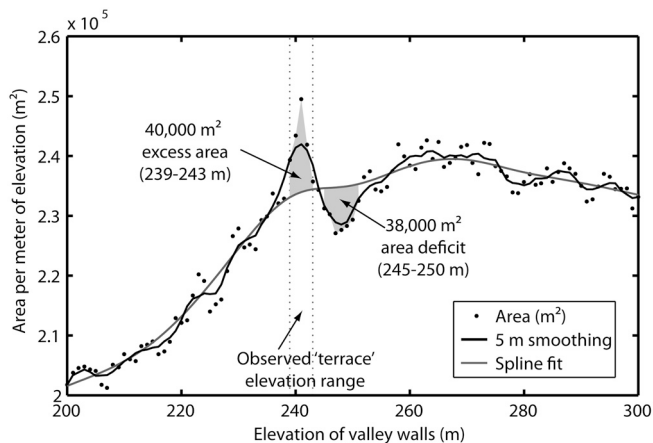

Fig. 2. LiDAR-derived hypsometry of 200- to 300-m elevation interval along Eel River upstream of the dam location. Area is binned per meter of elevation and shows a peak at 239–243 m, the elevations where terrace features are observed.
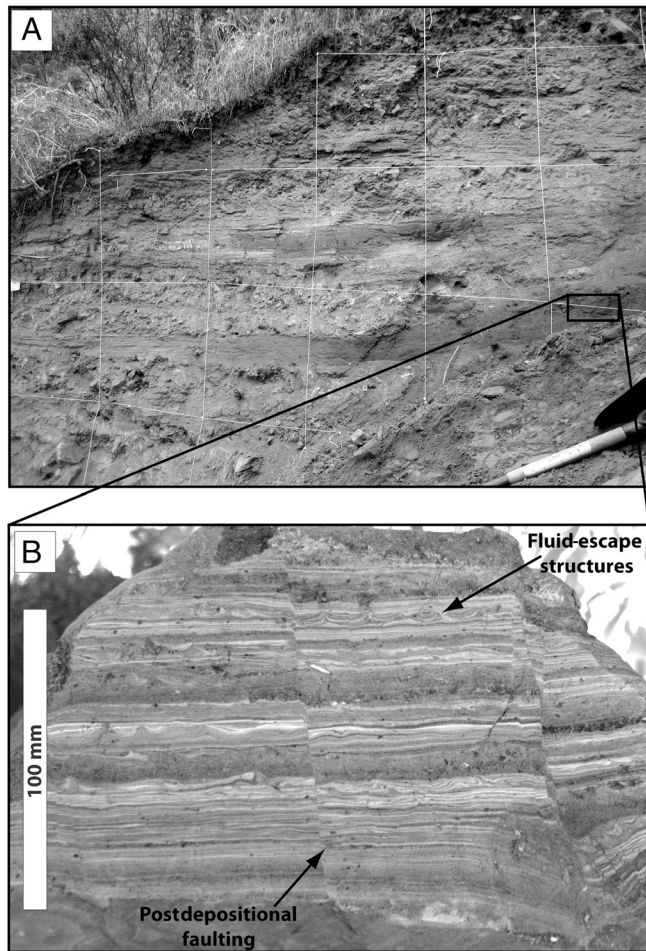
Fig. 3. Location of landslide scar and approximate dam location shown on a LiDAR-derived blended hillshade and slope map. Inset graphs show cross-section of landslide scar and the modern valley at the dam location used to calculate potential outburst-flood magnitude. Coordinates are Universal Transverse Mercator Zone 10N.

mately 0.5 mm/y) (14), the Eel River may have incised 10–15 m below the predam river bed elevation since the damming episode. The adjacent hillslopes likely have responded to a similar degree through earthflow activity, decreasing the chances of finding evidence for the dam (or terraces and lake deposits) in situ, whereas the landslide scar persists because of the erosion-resistant greenstone.

We analyzed the volume and extent of the lake from LiDAR data augmented with 10-m resolution digital topography. Assuming Nefus Peak is the source of the dam and a lake level of 240 m, the paleolake covered an area of 29 km^2 and had a volume of 1.3 km^3 based on modern topography (Fig. 1B). The dam catchment area was approximately 5,500 km^2, which accounts for 58% of the modern Eel River watershed, and enclosed the bulk of the highly erodible Central Belt Mélange rock in the catchment (25, 32). In comparison to most landslide dams that occur in steep mountainous topography with high gradient rivers (33, 34), the Eel River and adjacent hillslopes have relatively low gradients (0.003 and 0.3–0.35, respectively), such that the paleolake was vast, extending approximately 55-km upstream (Fig 1 and Fig. S4). The Eel River currently has an average annual water discharge of 6.6 km^3/y (2), indicating the lake would have filled with water in weeks or months in the wetter late Pleistocene climate (21, 35). Given an erosion rate of 0.5 mm/y and assuming complete retention of sediment behind the dam, the lake would

have filled with sediment in about 600 y, or within 6,000 y accounting only for bedload impoundment (13).

Although evidence indicating how the dam failed is currently lacking, large landslide dams frequently fail catastrophically via mass failure, overtopping, or piping (33, 34), and they are particularly vulnerable in tectonically active areas such as the Eel River catchment. We estimate the maximum potential outburst-flood discharge from the paleolake assuming complete catastrophic failure of the dam and critical flow through the breach; a reasonable approach given the relatively large lake volume (34). Gradual erosion of the dam or infilling of the lake with sediment could have produced a lesser discharge. We estimate the breach geometry from the modern valley cross-section at the narrowest point in the valley below the landslide (Fig. 3). Assuming failure of a 130-m-tall dam, peak discharge is approximately 8.4×10^5 m^3/s through the 610-m-wide and 101-m-deep channel, comparable to other outburst floods from lakes of this depth and volume (34). This discharge approximates the water transport capacity of the channel at this location for steady and uniform flow. Due to the size of the impoundment and volume of the lake, this potentially represents the second largest documented landslide dam outburst flood in North America (34).

Further evidence for the dam comes from an anomalously low concentration of Eel River derived sediments recorded offshore in an interval from 25 to 22 ka (16). Previously, oceanic circulation patterns were proposed as the cause of these sedimentary

Fig. 4. (*A*) Outcrop of lacustrine deposits exposed on the southern bank of Kekawaka Creek (see Fig. 3 for location). Grid scale is 0.5 m. Matrix supported, poorly sorted angular gravels separate the fine-grained laminated sequences. (*B*) Sample of finely laminated deposits near the base of the section. The absence of mud cracks suggests no subaerial exposure during deposition, whereas fluid-escape structures and the absence of bioturbation indicate rapid deposition.

records, as a shutdown of Eel River sedimentation was envisioned as highly unlikely (16). Because the age of the lake deposits fall within the interval during which the low sediment yield was recorded, we propose the landslide-dammed lake arrested much of the flux of sediment down the Eel River (as is common for large dammed lakes). This period of suppressed Eel River sediment delivery represents an important example of a discrete terrestrial signal transmitted through the fluvial system and recorded in the marine record. Given the Eel River catchment's high erosion rate, short river length, minimal floodplain, and proximal offshore depocenter (2), it is well suited to both rapidly transmit terrestrial perturbations and preserve them in the marine environment (29).

The landslide dam also provides an explanation for local genetic divergence of anadromous trout. Like many catchments in western North America, the Eel River has two reproductive ecotypes of anadromous Pacific Steelhead trout (*Oncorhynchus mykiss*). The endangered summer run steelhead migrate upriver from April to July and reside in deep pools in the upper Middle Fork Eel River (Fig. 1*B*), before spawning in the winter (22, 36). Winter run steelhead migrate upriver during winter months and spawn across much of the Eel River shortly thereafter. The two reproductive ecotypes can interbreed, but the populations are normally geographically isolated, with summer run fish spawning

farther upriver. Distinct to the Eel River, the ecotypes are more closely related to each other than equivalent ecotype comparisons in nearby rivers, suggesting a local cause rather than regional climatic or tectonic forcing (22, 37). Assuming summer and winter run steelhead populations existed in the Eel River prior to the landslide (as in adjacent catchments), the landslide dam can explain the recent (16–28 ka) apparent genetic divergence of the steelhead (22), owing to genetic introgression while the dam was emplaced. The landslide dam would likely have been impassable to anadromous fish, blocking access to the Middle Fork Eel River spawning grounds. Returning summer and winter run steelhead would have been forced to spawn in the river below the dam, allowing gene flow between the reproductive ecotypes, potentially for centuries or longer, resulting in more closely related ecotypes than in adjacent river systems. Although events such as drainage capture have been shown to cause genetic divergence in freshwater fish (38), and there are examples of natural dams blocking anadromous fish passage (10), genetic introgression (hybridization) is considerably rarer, and there are few documented examples that do not involve anthropogenic modification of the environment or species relocation.

Conclusions

Extreme geomorphic events can drive fundamental change to both landscapes and ecosystems, although it is rare to be able to clearly and directly point to how a specific prehistoric event, such as a large landslide, ultimately manifests in the landscape and depositional record, or may drive genetic change in animals. This difficulty arises because evidence for the event can be rapidly removed or comprise one of many similar events or signals so as to be nonunique. Because evidence for a landslide dam of this size and duration is rare in the Eel River environment (39), we are able to isolate the dam's effects on the landscape, and we link the cessation of sedimentation to marine sediments. The Eel River landslide dam represents a rare example of a discrete and transient geologic event permanently affecting a population of anadromous fish (10), and it may serve as a useful analogue for the long-term genetic effect of engineered dams on modern fish populations. Finally, a 130-m-tall landslide dam and 55-km-long lake represents a fundamental geomorphic feature and significant potential hazard. The combination of a wetter late Pleistocene climate (35) and seismic activity is an appealing explanation for the original failure of the landslide, although this remains speculation. Smaller examples of landslide-dammed lakes are not uncommon in steep mountainous terrain; however, landslide-dammed paleolakes of this scale are comparatively rare in low-relief, low-gradient landscapes with weak, highly sheared *meta*-sedimentary rocks. These environmental conditions are common to many parts of the Pacific Rim and southern Europe, where the potential hazard and geomorphic role of landslide-dammed lakes may be underestimated.

Materials and Methods

Terraces. We used LiDAR-derived maps and shoreline shape files loaded onto a handheld Global Positioning System unit to accurately follow the potential paleolake shore along contour for kilometers at a time. Along these transects, we used a combination of hand auger, soil pits, and investigation of the banks of incised streams to look for lakeshore deposits.

Fig. 2 was constructed by binning the total area within each meter of elevation along the main stem Eel River and tributaries to construct a graph of the canyon elevation hypsometry for 28-km upstream of the potential dam site to the confluence with the North Fork Eel (the extent of the LiDAR coverage). We analyzed the elevation range 200–300 m because this generously bracketed the targeted terrace elevation, yet avoided the broad (100- to 150-m wide) bed of the Eel River.

Lacustrine Deposits. The outcrop of lacustrine sediments was perched behind a large rock pinnacle approximately 10 m above the present elevation of Kekawaka Creek, and it had been recently exposed by a slump. We excavated several 20 cm a side cubic blocks of fine-grained sediments for detailed

analysis, and identified wood, bark, and submillimeter scale charcoal fragments using a binocular microscope. For the charcoal samples, multiple fragments along a discrete horizon were aggregated to obtain sufficient mass (>0.005 g) for radiocarbon dating. Two samples were processed and analyzed by Beta Analytic. We pretreated the remaining three samples in the Archaeometry Facility in the Department of Anthropology, University of Oregon. Samples and standards (process and background) were pretreated using standard acid-alkali-acid procedures, sealed in quartz tubes under vacuum, and combusted to CO_2 gas. The samples were then submitted to the Center for Accelerator Mass Spectrometry at The Lawrence Livermore National Laboratory for graphitization and accelerator mass spectrometer analysis.

Landslide Scar. We calculated the minimum volume of the landslide scar by rubber-sheeting a surface over the margins of the landslide scar and calculating the volume between this surface and the LiDAR-derived topography. To estimate the size of the dam, we calculated the volume required to fill the current Eel River canyon topography to 240 m, with upstream- and downstream-facing slopes at an angle of 18° (mean of adjacent hillslopes).

Outburst Flood. Using the Bernoulli equation for conservation of energy, h_c is the height of the water flowing through the breach, and H is the depth of the lake near the dam ($H = 130$ m). We can estimate h_c from (40)

$$h_c = H - \frac{Q^2}{2gA^2},\qquad [1]$$

where Q is discharge (cubic meters per second), g is acceleration of gravity (9.8 m/s^2), and A is the cross-sectional area of flow (square meters).

Assuming critical flow just downstream of the breach such that the Froude number (Fr) = 1,

$$Fr = \left[\frac{Q^2 w}{gA^3}\right]^{\frac{1}{2}} = 1,\qquad [2]$$

where w is the width at the top of the flow. Combining the above equations, we can iterate with the Eel River topographic cross-section (Fig. 3) to find $h_c = 101$ m, $A = 35,000$ m^2, $w = 610$ m, and $Q = 8.4 \times 10^5$ m^3/s.

Applying Manning's equation for channel water flow capacity (Q_n),

$$Q_n = \frac{A\left(\frac{A}{P}\right)^{\frac{2}{3}}S^{\frac{1}{2}}}{n},\qquad [3]$$

where P is the wetted perimeter (670 m), S is the bed slope (0.003), and n is Manning's roughness coefficient (0.03–0.06), gives a range of Q_n of 4.5 to 9.0×10^5 m^3/s. This analysis suggests the channel is able to carry the critical flow (Q), at least at steady and uniform flow conditions.

1. Sommerfield CK, Wheatcroft RA (2007) Late Holocene sediment accumulation on the northern California shelf: Oceanic, fluvial, and anthropogenic influences. *Geol Soc Am Bull* 119:1120–1134.
2. Wheatcroft RA, Sommerfield CK (2005) River sediment flux and shelf sediment accumulation rates on the Pacific Northwest margin. *Cont Shelf Res* 25:311–332.
3. Blair NE, et al. (2003) The persistence of memory: The fate of ancient sedimentary organic carbon in a modern sedimentary system. *Geochim Cosmochim Acta* 67:63–73.
4. Reimchen TE (2000) Some ecological and evolutionary aspects of bear-salmon interactions in coastal British Columbia. *Can J Zool* 78:448–457.
5. Korup O (2006) Rock-slope failure and the river long profile. *Geology* 34:45–48.
6. Korup O, Densmore AL, Schlunegger F (2010) The role of landslides in mountain range evolution. *Geomorphology* 120:77–90.
7. Restrepo C, et al. (2009) Landsliding and its multiscale influence on mountainscapes. *Bioscience* 59:685–698.
8. Ouimet WB, Whipple KX, Crosby BT, Johnson JP, Schildgen TF (2008) Epigenetic gorges in fluvial landscapes. *Earth Surf Processes Landforms* 33:1993–2009.
9. Korup O, Montgomery DR, Hewitt K (2010) Glacier and landslide feedbacks to topographic relief in the Himalayan syntaxes. *Proc Natl Acad Sci USA* 107:5317–5322.
10. Zimmerman CE, Ratliff DE (2003) Controls on the Distribution and Life History of Fish Populations in the Deschutes River: Geology, Hydrology, and Dams. *Geology and Geomorphology of the Deschutes River, Oregon*, Water Science and Application, eds JE O'Connor and GE Grant (Am Geophysical Union, Washington, DC), 7, pp 51–70.
11. Safran EB, Anderson SW, Mills-Novoa M, House PK, Ely LL (2011) Controls on large landslide distribution and implications for the geomorphic evolution of the southern interior Columbia River basin. *Geol Soc Am Bull* 123:1851–1862.
12. Kelsey HM (1978) Earthflows in Franciscan Melange, Van Duzen River Basin, California. *Geology* 6:361–364.
13. Brown WM, Ritter JR (1971) Sediment transport and tubidity in the Eel River basin, California. *US Geological Survey Water-Supply Paper*, 1986 (US Geological Survey, Washington, DC) p 67.
14. Mackey BH, Roering JJ (2011) Sediment yield, spatial characteristics, and the long-term evolution of active earthflows determined from airborne LiDAR and historical aerial photographs, Eel River, California. *Geol Soc Am Bull* 123:1560–1576.
15. Sloan J, Miller JR, Lancaster N (2001) Response and recovery of the Eel River, California, and its tributaries to floods in 1955, 1964, and 1997. *Geomorphology* 36:129–154.
16. VanLaningham S, Duncan RA, Pisias NG, Graham DW (2008) Tracking fluvial response to climate change in the Pacific Northwest: A combined provenance approach using Ar and Nd isotopic systems on fine-grained sediments. *Quat Sci Rev* 27:497–517.
17. Sommerfield CK, Drake DE, Wheatcroft RA (2002) Shelf record of climatic changes in flood magnitude and frequency, north-coastal California. *Geology* 30:395–398.
18. Nittrouer CA (1999) STRATAFORM: Overview of its design and synthesis of its results. *Mar Geol* 154:3–12.
19. Kelsey HM, Carver GA (1988) Late Neogene and quaternary tectonics associated with northward growth of the San-Andreas Transform-Fault, Northern California. *J Geophys Res Solid Earth Planets* 93:4797–4819.
20. Merritts DJ (1996) The Mendocino triple junction: Active faults, episodic coastal emergence, and rapid uplift. *J Geophys Res Solid Earth* 101:6051–6070.
21. Syvitski JP, Morehead MD (1999) Estimating river-sediment discharge to the ocean: Application to the Eel margin, northern California. *Mar Geol* 154:13–28.
22. Nielsen JL, Fountain MC (1999) Microsatellite diversity in sympatric reproductive ecotypes of Pacific steelhead (*Oncorhynchus mykiss*) from the Middle Fork Eel River, California. *Ecol Freshw Fish* 8:159–168.
23. Seidl MA, Dietrich WE (1992) The problem of channel erosion into bedrock. *Catena Supp* 23:101–124.
24. Fuller TK, Perg LA, Willenbring JK, Lepper K (2009) Field evidence for climate-driven changes in sediment supply leading to strath terrace formation. *Geology* 37:467–470.
25. McLaughlin RJ, et al. (2000) Geology of the Cape Mendocino, Eureka, Garberville, and Southwestern part of the Hayfork 30 × 60 Minute Quadrangles and Adjacent Offshore Area, Northern California. (US Geological Survey, Denver) Miscellaneous Field Studies Map MF-2336.
26. Cruden DM, Varnes DJ (1996) Landslide types and processes. *Landslides: Investigation and Mitigation*, eds AK Turner and RL Schuster (Natl Academy Press, Washington, DC), pp 36–71 Vol National Research Council, Special Report 247.
27. Pratt-Sitaula B, et al. (2007) Bedload-to-suspended load ratio and rapid bedrock incision from Himalayan landslide-dam lake record. *Quat Res* 68:111–120.
28. Montgomery DR, et al. (2004) Evidence for Holocene megafloods down the Tsangpo River Gorge, southeastern Tibet. *Quat Res* 62:201–207.
29. Allen JRL (1985) *Principles of Physical Sedimentology* (Allen & Unwin, London) p 272.
30. Lamb MP, McElroy B, Kopriva B, Shaw J, Mohrig D (2010) Linking river-flood dynamics to hyperpycnal-plume deposits: Experiments, theory, and geological implications. *Geol Soc Am Bull* 122:1389–1400.
31. Fairbanks RG, et al. (2005) Radiocarbon calibration curve spanning 0 to 50,000 years BP based on paired Th-230/U-234/U-238 and C-14 dates on pristine corals. *Quat Sci Rev* 24:1781–1796.
32. Jayko AS, et al. (1989) Reconnaissance Geologic Map of the Covelo 30- by 60- Minute Quadrangle, Northern California. (US Geological Survey, Reston, VA) Miscellaneous Field Studies Map 2001.
33. Costa JE, Schuster RL (1988) The formation and failure of natural dams. *Geol Soc Am Bull* 100:1054–1068.
34. O'Connor JE, Beebee RA (2009) Floods from natural rock-material dams. *Megaflooding on Earth and Mars*, eds DM Burr, PA Carling, and VR Baker (Cambridge Univ Press, New York), pp 128–163.
35. Adam DP, West GJ (1983) Temperature and precipitation estimates through the last glacial cycle from Clear Lake, California, pollen data. *Science* 219:168–170.
36. Nielsen JL, Lisle TE, Ozaki V (1994) Thermally stratified pools and their use by steelhead in Northern California streams. *Trans Am Fish Soc* 123:613–626.
37. Montgomery DR (2000) Coevolution of the Pacific salmon and Pacific Rim topography. *Geology* 28:1107–1110.
38. Waters JM, et al. (2007) Geological dates and molecular rates: Rapid divergence of rivers and their biotas. *Syst Biol* 56:271–282.
39. Muhs DR, et al. (1987) Pacific Coast and Mountain System. *Geomorphic Systems of North America*, ed WL Graf (Geological Soc America, Boulder, CO), Vol Centennial Special Vol 2, pp 517–581.
40. Chow VT (1959) *Open-Channel Hydraulics* (McGraw-Hill, New York), pp 40–59.

GEOLOGY

EVOLUTION

Supporting Information
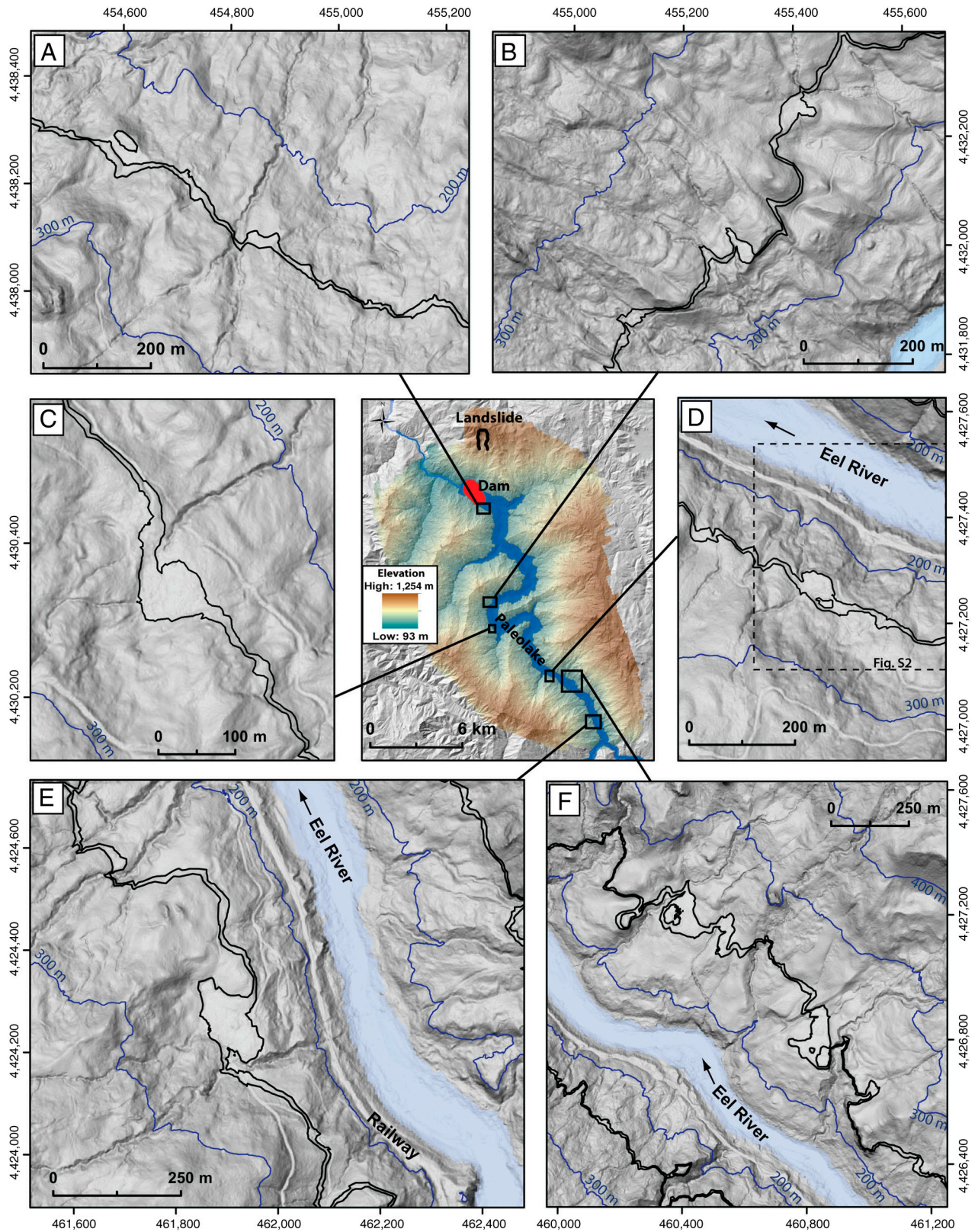
Mackey et al. 10.1073/pnas.1110445108

Fig. S1. Examples of gently sloping terrace-like features at 240- to 243-m elevation, with respect to the Eel River paleolake (*Center*). Black lines are 240 and 243 m contours. Colored elevation in center pane indicates extent of Light Detection and Ranging dataset coverage. Coordinates are Universal Transverse Mercator Zone 10N.
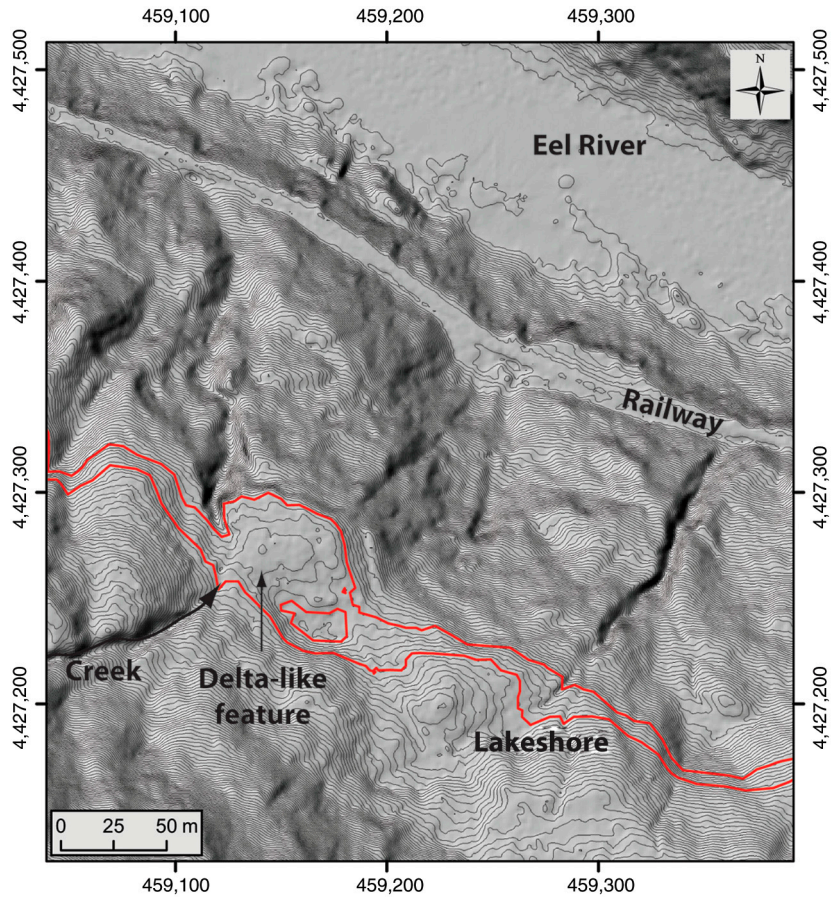

Fig. S2. Delta-like feature where a creek entered the inferred paleolake, indicated by the gently convex topography where the creek meets the paleoshoreline. Location is shown in Fig. S1*D*. Red lines are 240 and 243 m contours, and black lines are 0.5 m contour intervals. Coordinates are Universal Transverse Mercator Zone 10N.
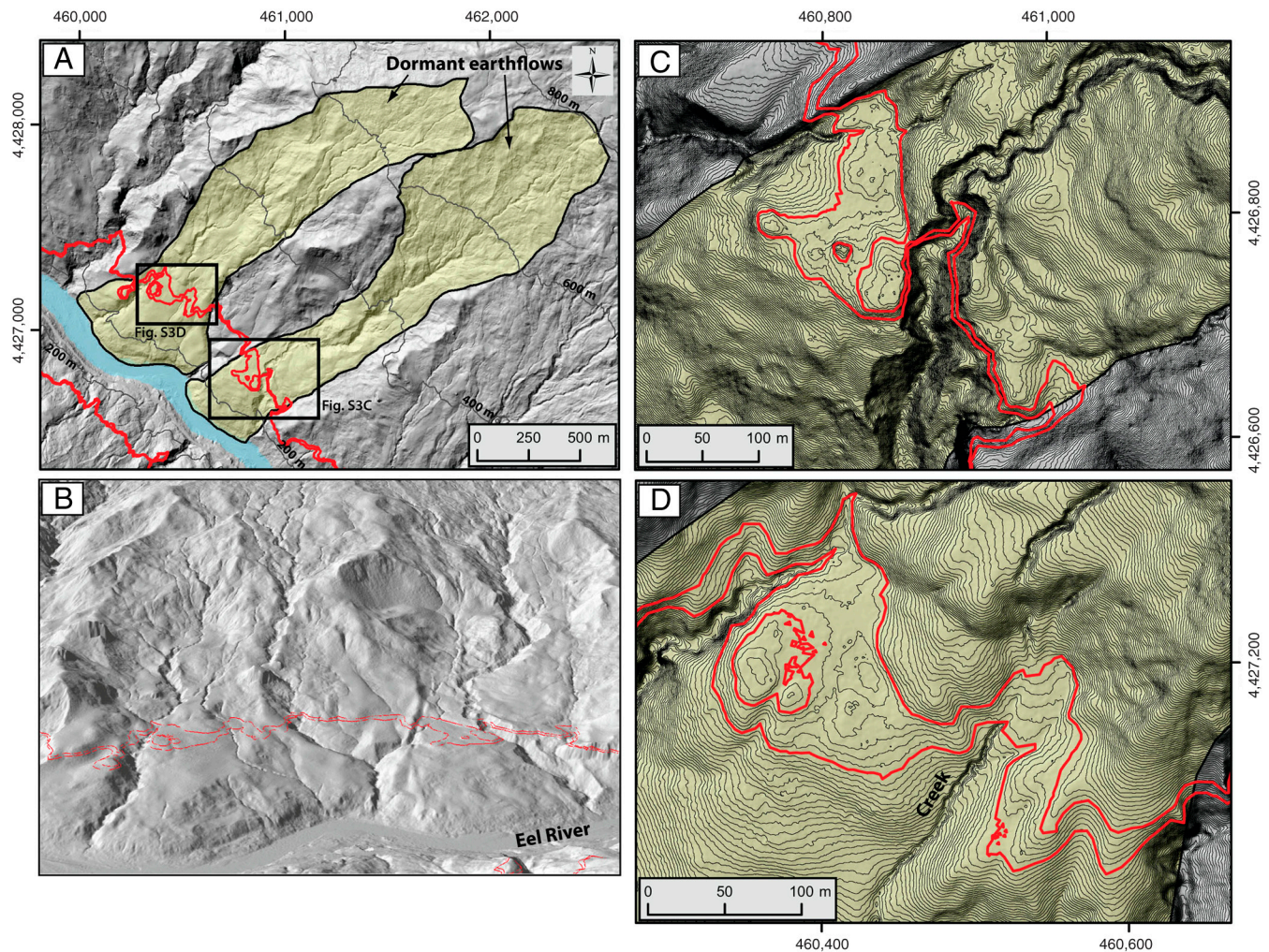
Fig. S3. (*A*) Two large earthflows (yellow shading) which have been dormant in historic times (1) exhibit paleolake shorelines cut into their surface. Because the shoreline features (also shown in Fig. S1*F*) would likely be translated and erased by earthflow movement, it suggests the earthflows have not been active for at least 22 ka, a rare constraint on the activity of large earthflows. Red lines are 240 and 243 m contours, coordinates are Universal Transverse Mercator Zone 10N. (*B*) Oblique view of shaded relief Light Detection and Ranging dataset topography looking northeast across the Eel River at the dormant earthflow toes— red lines are 240 and 243 m contours. (*C* and *D*) Close up of the southern (*C*) and northern (*D*) earthflows at the elevation of the lake shoreline. Contour interval is 0.5 m. Red lines are 240 and 243 m contours. Note the broad gently sloping regions on the earthflow surfaces at the elevation of the lakeshore in comparison to the adjacent hummocky earthflow surface. We interpret these bench-like features to represent deposition of sediments and potentially wave cutting indicated by the steep slopes from 244 to 250 m.

1 Mackey BH, Roering JJ (2011) Sediment yield, spatial characteristics, and the long-term evolution of active earthflows determined from airborne LiDAR and historical aerial photographs, Eel River, California. *Geol Soc Am Bull* 123:1560–1576.
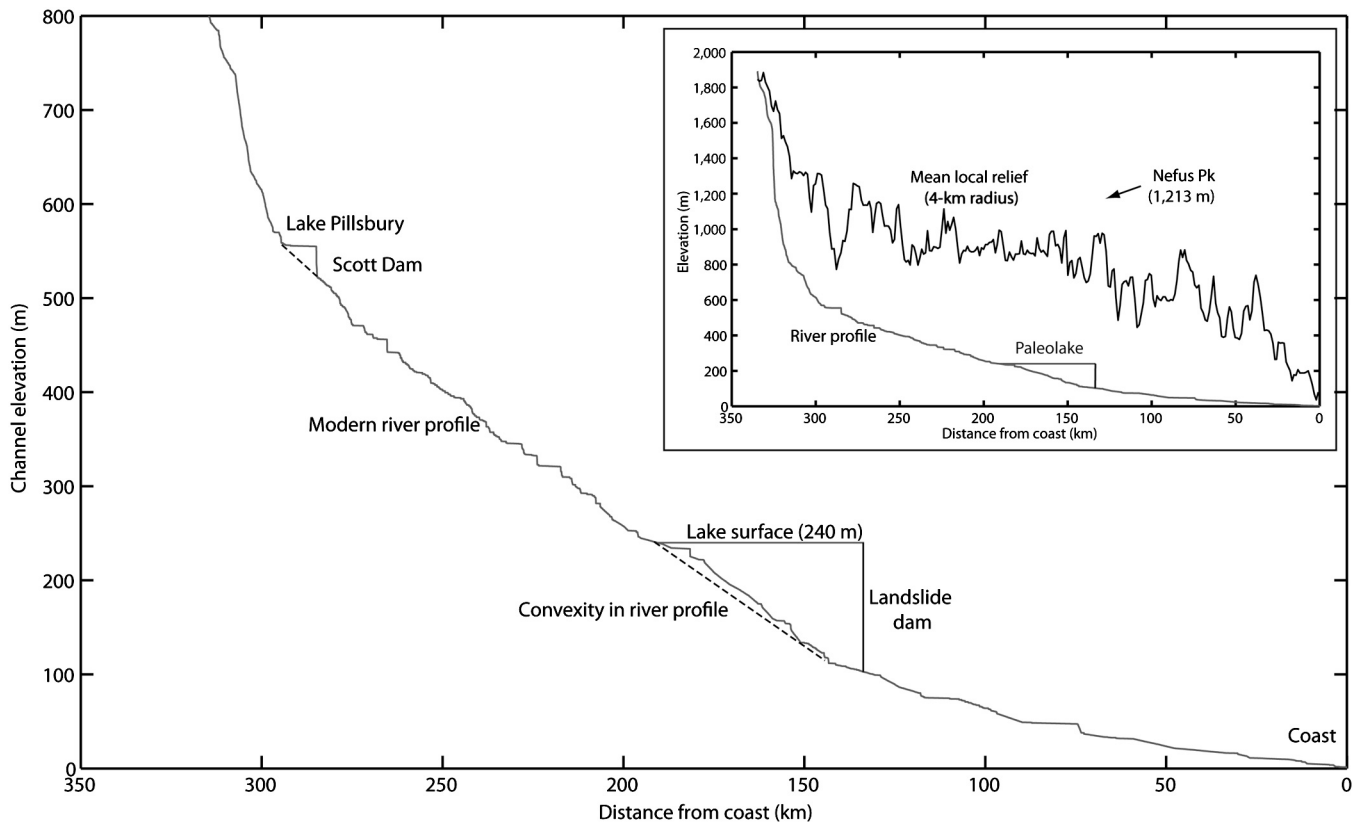
Fig. S4. Lower Eel River long profile extracted from US Geological Survey 10 m Digital Elevation Model (1) (data available from US Geological Survey) showing location of landslide dam and projected lake surface. The long profile has a slight convexity in the upper section of the paleolake, possibly attributable to sediment aggradation while the lake was emplaced, or arming of the channel bed by sediment or water. Lake Pillsbury (upstream) is a man-made lake. The inset shows the full Eel River profile in addition to mean local relief along the main stem Eel River. Mean local relief is defined as the elevation range within a circle of 4-km radius, the approximate length of the river to bounding-ridge distance along the Eel River. There is little remaining evidence of the dam itself on the river profile or in the field (e.g., preserved dam abutments, large rocks in the creek). Local reports suggest there were formerly rapids or falls at the dam location, although many of the larger rocks in the river were blown up during construction of a railway line adjacent to the Eel River, to prevent eddies from undermining the tracks (2).

1 Gesch D, et al. (2002) The National Elevation Dataset. *Photogramm Eng Remote Sens* 68:5–11.
2 Mathison R (1998) *The History of Alderpoint* (Eureka Printing, Eureka, CA), pp 50–51.

Table S1. Sediment radiocarbon ages

Sample ID	Lab	Lab ID	Sample description	Source	^{14}C age, year	Error (±1 σ)	Calendar age, year	Error (±1 σ)
KW 1 C	CAMS	144,860	bark	paleosol	210	30	230	80
KW 3-1	CAMS	144,861	detrital charcoal	laminated silts	21,440	80	25,745	154
KW 4-1	CAMS	144,862	detrital charcoal	laminated silts	19,020	60	22,592	95
KW2:8	Beta	Beta-256,979	detrital charcoal	laminated silts	36,050	300	41,306	320
KW2:9	Beta	Beta-256,980	wood	laminated silts	80	40	N/A	N/A

Radiocarbon and calendar ages (1) of samples in fine-grained lacustrine deposits. CAMS, Center for Accelerator Mass Spectrometry at Lawrence Livermore National Laboratory; Beta, Beta Analytic.

1 Fairbanks RG, et al. (2005) Radiocarbon calibration curve spanning 0 to 50,000 years BP based on paired Th-230/U-234/U-238 and C-14 dates on pristine corals. *Quat Sci Rev* 24:1781–1796.